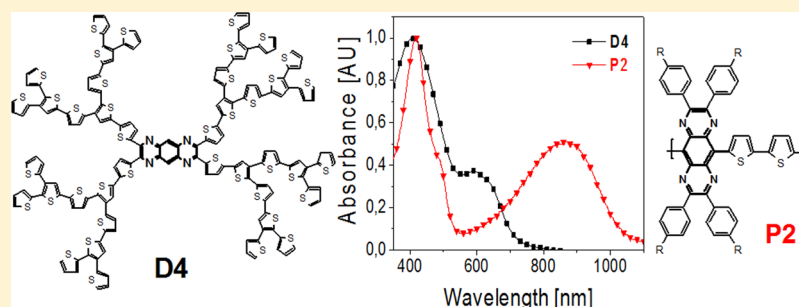


Synthesis and Photovoltaic Performance of Pyrazinoquinoxaline Containing Conjugated Thiophene-Based Dendrimers and Polymers

Gisela L. Schulz,^{*,‡} Michael Mastalerz,[‡] Chang-Qi Ma,^{‡,§} Martijn Wienk,[†] René Janssen,[†] and Peter Bäuerle^{*,‡}[†]Nanosystems, Eindhoven University of Technology, P.O. Box 513, 5600 MB Eindhoven, The Netherlands[‡]Institute of Organic Chemistry II and Advanced Materials, University of Ulm, Albert-Einstein-Allee 11, D-89081 Ulm, Germany

Supporting Information



ABSTRACT: Pyrazinoquinoxaline-based building blocks were incorporated into both π -conjugated dendrimers and polymers. The dendrimers were synthesized using a convergent/divergent approach whereas the donor/acceptor copolymers were synthesized via Stille cross-coupling reactions. The structurally defined dendrimers and the π -conjugated polymers were investigated with respect to their optical and electronic properties as well as their performance in photovoltaic devices. Because of the presence of the electron-deficient pyrazinoquinoxaline moiety, the absorption spectra of the materials under investigation were red-shifted with respect to the all thiophene-containing materials. Power conversion efficiencies up to 1.7 and 0.8% were obtained from blends of second-generation dendrimers and polymers with PC₇₁BM, respectively.

INTRODUCTION

Over the past decades, there has been increasing interest in the development of new materials for applications in organic bulk heterojunction solar cells (BHJSC).^{1–3} The field has been expanding rapidly with the number of new compounds being produced at an increasingly faster rate.^{4,5} The materials investigated to date can be classified into the following four categories: conjugated polymers, dendrimers, oligomers, and small dye molecules. This work reports on the synthesis and structure–property relationships of two of the above classes of materials, i.e., π -conjugated dendrimers and polymers, for use as electron donors in fullerene-based BHJSCs.

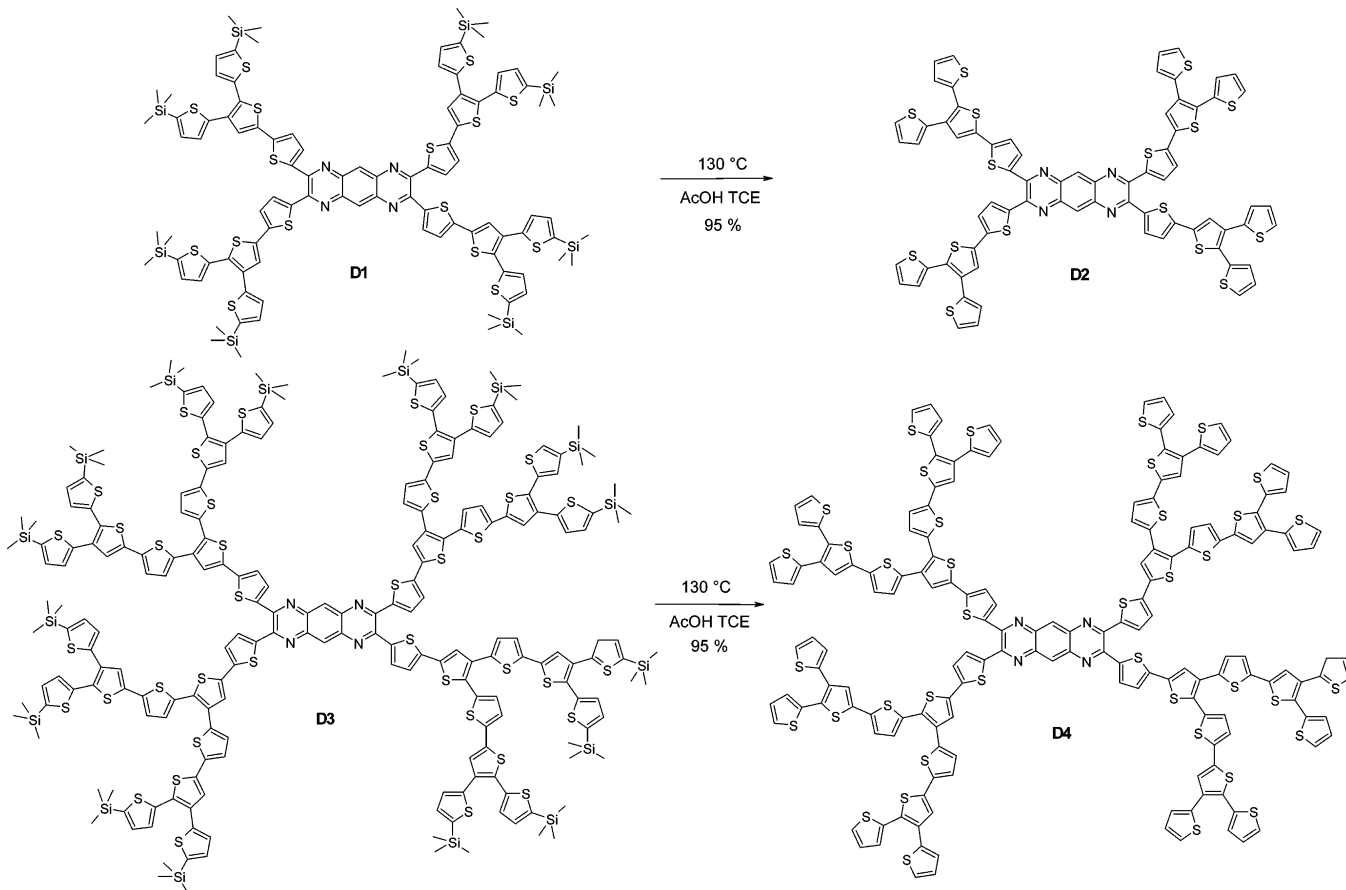
Shape-persistent molecules such as conjugated dendrimers are of interest for applications in photovoltaics because of their defined structure, monodispersity, and the possibility to derive structure–property relationships. Problems with respect to reproducibility of results due to batch to batch differences, such as in the case of polymers, are of less significance. Challenges in the field of dendrimers lie in the synthesis and most frequently in the purification of the often large molecules. Several groups have reported on dendritic systems and their performance in BHJSCs. Roncali et al. investigated triphenylamine-based molecules end-capped with dicyanovinylene, yielding power conversion efficiencies (PCEs) up to 1.85% in bilayer solar cells.⁶ A very similar molecule was reported by Zhang and co-

workers, in which a vinylene group was incorporated between the phenyl and thiophene moieties. In this case the authors were able to improve the PCEs to 3.0% when they blended the star-shaped triphenylamine with [6,6]-phenyl-C₇₁-butyric acid methyl ester (PC₇₁BM, 1:2).⁷ Furthermore, Kopidakis and co-workers increased the PCE of an X-shaped thiophene-based dendrimer via core-functionalization upon addition of electron-withdrawing cyano groups on the central benzene ring from 0.40 to 1.12%.⁸ Sun et al. reported on another X-shaped oligothiophene consisting of a tetrasubstituted thiophene core, that when blended with [6,6]-phenyl-C₆₁-butyric acid methyl ester (PC₆₁BM), showed an overall PCE of 0.8%.⁹ Based on work published by our group in 2008, wherein all-thiophene dendrimers up to the fourth generation were described, PCEs of up to 1.7% were reported for blends of a third-generation dendrimer containing 42 thiophene units (42T) with PC₆₁BM.^{10,11} Other dendrimer work by our group involved incorporating ruthenium(II) phthalocyanine complexes functionalized with dendritic oligothiophenes in the axial position, in bulk heterojunction solar cells. PCEs up to 1.7% were reported with blends consisting of RuPcCO(Py-3T) and

Received: November 21, 2012

Revised: February 28, 2013

Scheme 1. Deprotection of First- and Second-Generation Dendrimers D1 and D3 To Yield D2 and D4



PC₇₁BM.¹² Oligothiophene dendrimers incorporating ethynyl groups were also developed showing PCEs in the range of 0.4–0.8%.¹³ Furthermore, dendritic oligothiophene–perylene bisimide hybrid systems were synthesized and investigated with respect to their optoelectronic properties.¹⁴

A recent report from Tam et al. on the substituent effect on the electronic properties of pyrazino[2,3-*g*]quinoxaline molecules demonstrated the potential for fine-tuning the acceptor characteristics.¹⁵ With the aim of broadening the absorption spectrum and thereby increasing the number of harvested photons, we employed the same pyrazino[2,3-*g*]quinoxaline as electron-deficient moiety in the core of the dendritic molecules. A PCE of 1.3% was obtained for the 40T pyrazinoquinoxaline dendrimer (D3) with TMS protecting groups on the periphery of the molecule.¹⁶ The observed increase in PCE from 1.0 to 1.3%, when going from the protected 42T to 40T pyrazinoquinoxaline containing material, indicated the promising nature of this new series of thiophene dendrimers.¹¹

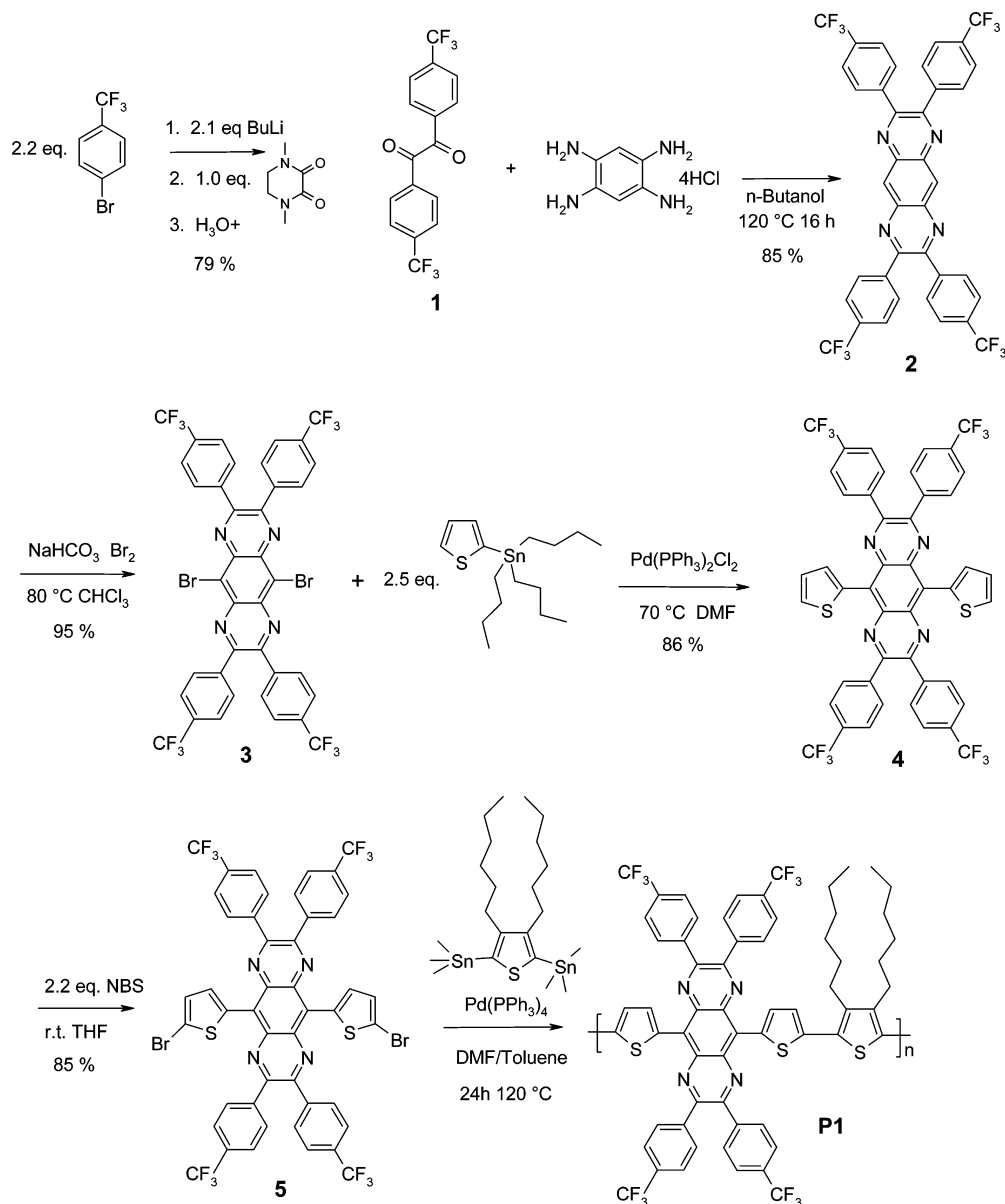
Using the knowledge gained from these dendrimeric systems, we then proceeded to design and synthesize conjugated polymers based on structurally similar building blocks. To date, there have been a few pyrazinoquinoxaline containing polymers published in the literature. A phenyl-substituted pyrazinoquinoxaline-*co*-fluorene polymer was reported by Zhang et al. which displayed a PCE of 1.7% with PC₆₁BM and 2.3% with PC₇₁BM.¹⁷ Shortly thereafter, Zoombelt et al. described two pyrazinoquinoxaline-*co*-thiophene polymers synthesized via Yamamoto cross-coupling. Of the two, the best performing polymer showed a PCE of 0.37% and 0.72% when blended with PC₆₁BM and PC₇₁BM, respectively.¹⁸

Additionally, Wang et al. synthesized a similar pyrazinoquinoxaline-*co*-thiophene using Stille cross-coupling and obtained a PCEs up to 2.1% with PC₇₁BM.¹⁹ Unver et al. also have described the electropolymerization of pyrazinoquinoxaline copolymers, wherein cyclic voltammetry and UV–vis–NIR absorption were investigated.²⁰ More recently, a series of pyrazinoquinoxaline-*co*-indolocarbazole polymers were reported by Peng et al. They measured PCEs up to 3.2% from polymer:PC₇₁BM blends.²¹ Herein, we report on the synthesis and characterization of four pyrazinoquinoxaline-based dendrimers and two donor/acceptor copolymers based on thiophene and pyrazinoquinoxaline alternating repeat units. Structure–property relationships and photovoltaic performances are discussed.

RESULTS

The pyrazinoquinoxaline-cored dendrimers D1 and D3 were synthesized using a previously reported method via a 4-fold Suzuki cross-coupling reaction between a tetra(bromothieryl)-pyrazinoquinoxaline and a terthiophene (3T)- or 9T-dendritic boronic ester to give the first- and second-generation dendritic oligothiophenes (DOT), respectively (Scheme 1).¹⁶ With respect to the removal of the TMS groups, we have previously shown that it occurs quantitatively for the all-thiophene dendrimers using tetrabutylammonium fluoride (TBAF).¹⁰ However, under the same conditions, we observed decomposition of the pyrazinoquinoxaline-based dendrimers. Multiple attempts were made to perform the deprotection, including the use of trifluoroacetic acid in dichloromethane (CH₂Cl₂), acetic acid (AcOH) in dichloromethane, trifluoroacetic acid in

Scheme 2. Synthetic Route Used To Obtain P1

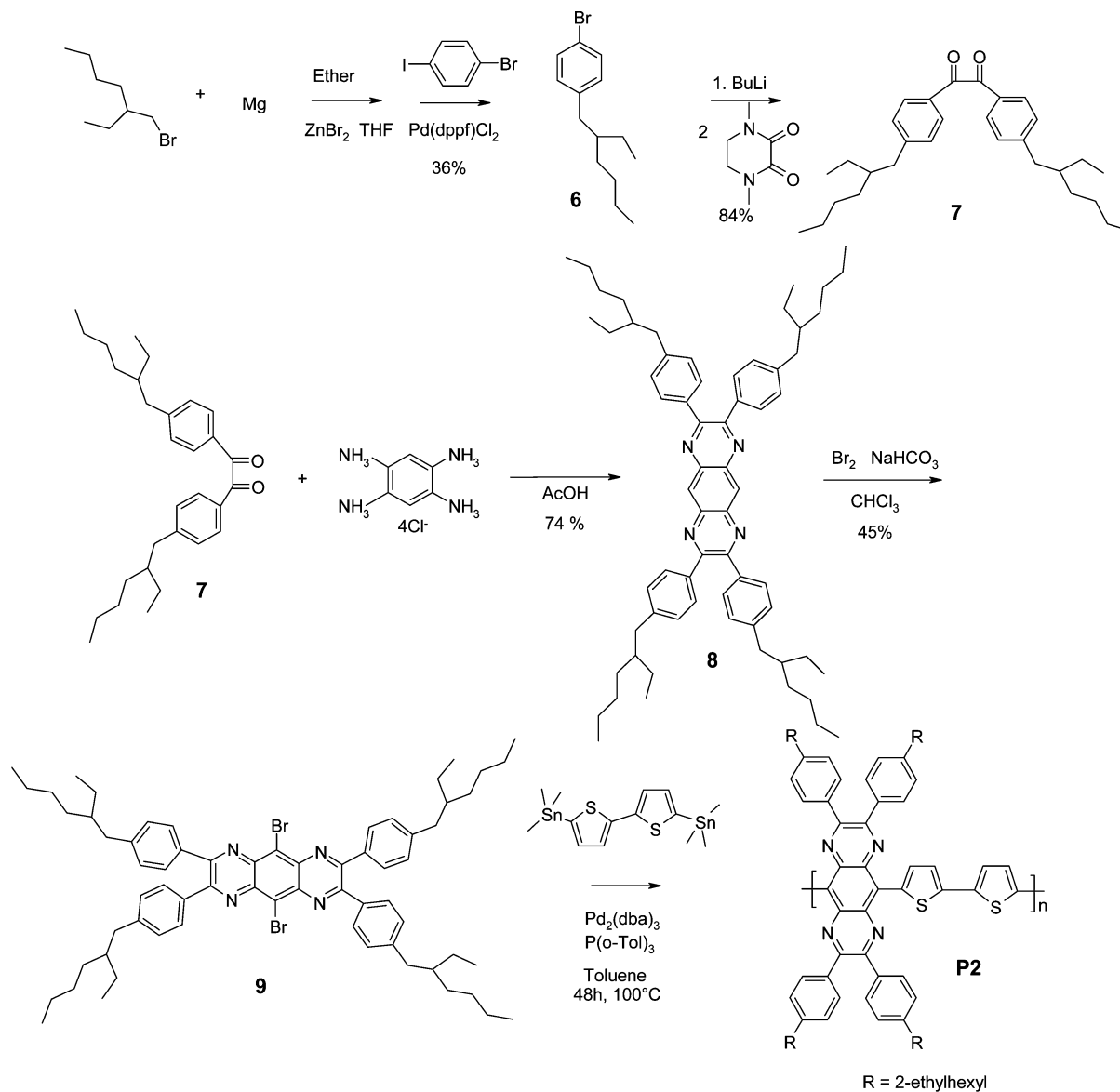


o-dichlorobenzene (ODCB), and simply neat acetic acid, all of which were unsuccessful. In general, deprotection using low boiling point solvents was also unsuccessful as higher temperatures were found to be necessary. This was later ascribed to the significantly reduced solubility of the product in comparison to the starting material. Solubility of **D2** and **D4** increased in the following solvents: CH_2Cl_2 < tetrahydrofuran (THF) < ODCB < 1,1,2,2-tetrachloroethane (TCE). An insoluble black solid was obtained when the reaction was carried out using trifluoroacetic acid. Finally, it was shown that the TMS groups could be cleaved in the presence of acetic acid and TCE after heating to 130 °C for 4 days. After work-up, the obtained solid was washed with pentane and methanol and then dried under vacuum to give the desired dendrimer in 95% yield.

The synthetic route used to obtain copolymer **P1** is shown in Scheme 2. The dimethylpiperazine-2,3-dione was reacted with the lithiated trifluorophenyl compound according to a known literature procedure to produce the desired diketone **1** in 79%

yield.²² The condensation of compound **1** with tetraaminobenzene tetrahydrochloride was performed in *n*-butanol under argon for 16 h and gave quinoxaline **2** in 85% yield. Compound **2** was further reacted with elemental bromine to yield the dibromo derivative **3** in 95% yield after recrystallization. Dibromopyrazinoquinoxaline (**3**) was further reacted with tributylstannylthiophene in order to obtain dithienylquinoxaline (**4**) in 86% yield. The desired dibrominated monomer **5** was synthesized by reacting **4** with NBS, followed by precipitation in methanol to give an overall yield of 85%. Polymer **P1** was successfully synthesized using Stille cross-coupling; the crude product was precipitated in MeOH and underwent successive Soxhlet extraction in MeOH, acetone, hexane, and THF. The THF fraction was then reprecipitated in methanol and dried under vacuum to yield **P1** in 48% yield. Molecular weight was estimated using gel permeation chromatography versus polystyrene standards, resulting in $M_n = 6300$ g/mol and $M_w = 8900$ g/mol, giving a PDI of 1.4. The

Scheme 3. Synthetic Route Used To Obtain P2



rather low molecular weight of **P1** is attributed to its poor solubility.

Scheme 3 depicts the synthetic route followed to obtain polymer **P2**. First, 1-bromo-4-(2'-ethylhexyl)benzene (**6**) was synthesized using Negishi cross-coupling to yield a colorless liquid in 36% yield. Compound **6** then underwent a metal-halogen exchange reaction with *n*-butyllithium, followed by quenching with dimethyl-piperazine-2,3-dione to produce **7**, in 84% yield, as described in a similar reaction in the literature.²² The condensation of compound **7** with tetraaminobenzene tetrahydrochloride was performed in acetic acid under argon for 24 h and gave the desired pyrazinoquinoxaline derivative, **8**, in 74% yield.

As depicted in Scheme 2, the trifluoromethyl analogue of **8**, derivative **2**, underwent bromination in the presence of 4 equivs. of elemental bromine, 4 equivs. of sodium hydrogen carbonate, and chloroform in 95% yield after reacting for 4 h at 80 °C. This unfortunately was not the case for the analogous reaction of **8** shown in Scheme 3. The bromination of **8** under the same conditions was more sluggish and less selective. After

some optimization, the desired product **9** could be obtained by first reaction of **8** with 2 equivs. of Br₂ and 2 equivs. of NaHCO₃ in CHCl₃ for 24 h at 80 °C, followed by cooling to room temperature and addition of another 2 equivs. of Br₂, 2 equivs. of NaHCO₃, and further reaction at 50 °C for 6 h. Dibromopyrazinoquinoxaline (**9**) was purified using silica gel chromatography, followed by recrystallization from THF/MeOH to yield bright orange crystals in 45% yield. From 5,10-dibromopyrazinoquinoxaline (**9**) and 2,5-bis-(trimethylstannyl)bithiophene, polymerization was carried out via a Stille cross-coupling reaction, as shown in Scheme 3. The crude product was precipitated in MeOH and underwent successive Soxhlet extraction in MeOH, acetone, hexane, and THF. The THF fraction was then reprecipitated in methanol and dried under vacuum to yield donor-acceptor polymer **P2** in 95% yield. Molecular weights were determined using gel permeation chromatography versus polystyrene standards, resulting in $M_n = 53\,000$ g/mol and $M_w = 113\,000$ g/mol, giving a PDI of 2.1.

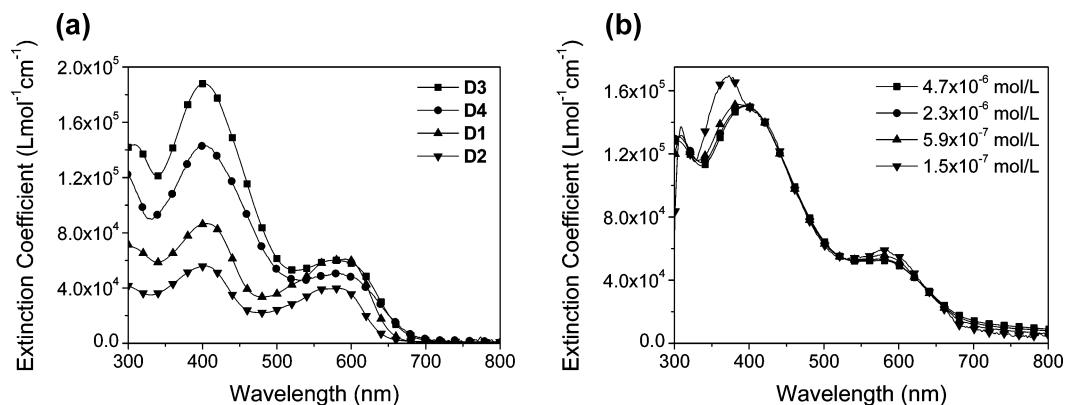


Figure 1. (a) UV-vis spectra of first- and second-generation dendrimers, with and without TMS protecting groups measured in TCE. (b) UV-vis spectra of D4 measured in TCE at various concentrations.

The UV-vis absorption spectra measured in TCE of the first- and second-generation dendrimers, with and without TMS groups, are displayed in Figure 1. Absorption in the high-energy region of the spectrum (between 350 and 500 nm) is attributed to the $\pi-\pi^*$ transition of the oligothiophene branches. It follows that this intensity should increase with longer oligothiophenes chains, i.e., upon increasing dendrimer generation. The intensity of the charge transfer band observed at longer wavelengths (~ 575 nm), comparatively, does not change its intensity upon increasing generation size; however, the onset is shifted from 643 nm for D2 to 679 nm for D4. The molar absorption coefficients of the pyrazinoquinoxaline containing DOTs are in the range 55 900–188 000 $\text{L mol}^{-1} \text{cm}^{-1}$. We observe an increase in extinction coefficient with increasing generation size (86 500 vs 188 000 $\text{L mol}^{-1} \text{cm}^{-1}$) for D1 and D3 as well as a small blue-shift in the absorption maximum from 410 to 400 nm, respectively. The second-generation deprotected dendrimer, D4, had the tendency to form aggregates in solution. This was observed in the broadness of the ^1H NMR peaks as well as in absorption spectra measured for various concentrations (see Figure 1b and Supporting Information). In Figure 1b, one can see the blue-shift of the absorption maximum, from 395 to 373 nm, as the concentration of D4 in TCE is reduced to $1.5 \times 10^{-7} \text{ mol L}^{-1}$.

The absorption spectra of thin films of the deprotected first- and second-generation dendrimers, D2 and D4, spin-coated from TCE, are displayed in Figure 2. Relative to measurements performed in solution, the absorption maximum and onset of the low-energy band of the D4 thin film displayed a red-shift of

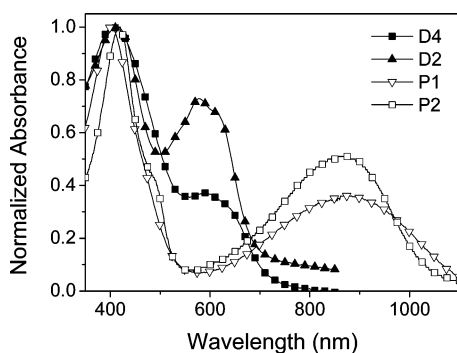


Figure 2. UV-vis spectra of D2, D4, P1, and P2 thin films. The dendrimer films were spin-coated from TCE and the polymers from CHCl_3 .

6 nm ($\lambda_{\text{max,soln}} = 581$ nm vs $\lambda_{\text{max,film}} = 587$ nm) and 45 nm ($\lambda_{\text{onset,soln}} = 675$ nm vs $\lambda_{\text{onset,film}} = 720$ nm), respectively. The absorption spectrum of D2 does not return to the baseline at longer wavelengths due to poor film-forming properties/solubility limitations which result in light scattering. As seen in the case for the measurements performed in solution, the thin films of the pyrazinoquinoxaline-cored DOTs have reduced absorption at 600 nm upon increasing dendrimer size. This is explained by the relative increase in donor content within dendrimer structure going from D2 to D4. Figure 2 also displays the absorption profiles of the thin films of polymers P1 and P2. Relative to the dendrimers, a significant red-shift in the charge transfer band is observed ($\lambda_{\text{CT,D4}} = 592$ nm vs $\lambda_{\text{CT,P1}} = 870$ vs $\lambda_{\text{CT,P2}} = 865$ nm) due to the different connectivity of pyrazinoquinoxaline unit to the thiophene moieties. In the case of the dendrimers, the donor thiophene units are bound to pyrazinoquinoxaline at the 2-, 3-, 7-, and 8-positions, whereas in the polymers the thiophene units are connected through the 5- and 10-positions. The latter is stabilized through the formation a quinoid resonance structure via intramolecular charge transfer resulting in the observed red-shift. The difference seen in the intensity of the longer wavelength absorption maxima of P1 and P2 is attributed to enhanced $\pi-\pi$ stacking in the film of P2 vs P1, likely due to the significantly higher molecular weight of P2 over P1 (53 000 vs 6000 g/mol).

In addition, we also performed fluorescence experiments in solvents with different polarity to determine the effect of the incorporation of the electron-deficient pyrazinoquinoxaline core on the dendritic molecules (see Figure 3). The emission

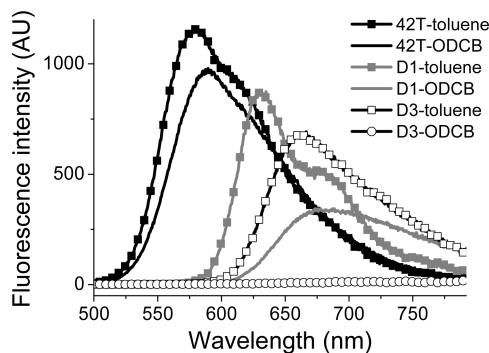


Figure 3. Fluorescence spectra of 42T, D1, and D3 in apolar toluene and polar *o*-dichlorobenzene (ODCB). Excitation wavelength was 400 nm for all measurements.

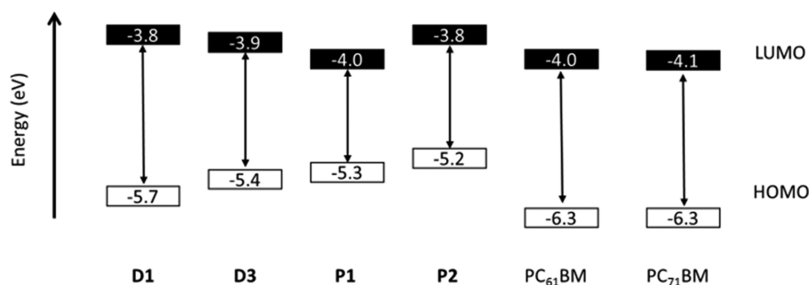


Figure 4. Energy level diagram (energy (eV) vs vacuum) showing the HOMO and LUMO levels of the dendrimers, polymers, and PCBM derivatives.^{23–25}

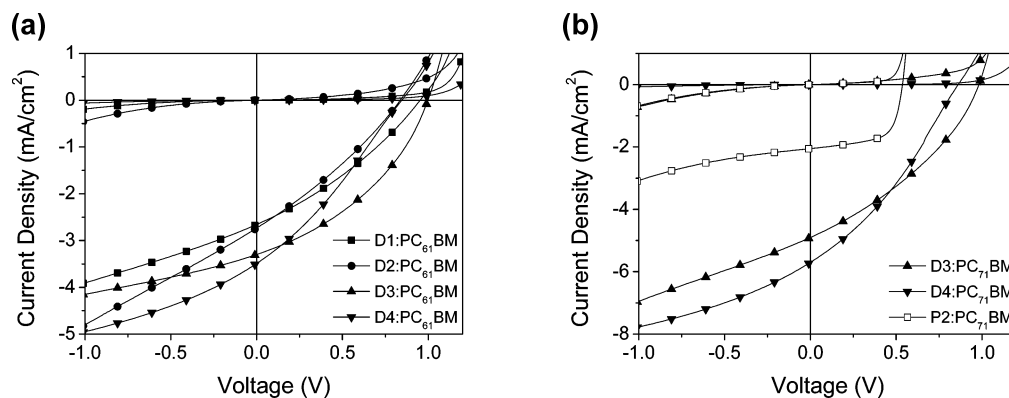


Figure 5. (a) J - V characteristics of **D1**, **D2**, **D3**, and **D4** blended with PC_{61}BM (1:3 ratio). (b) J - V characteristics of **D3**, **D4**, and **P2** blended with PC_{71}BM (1:3 ratio).

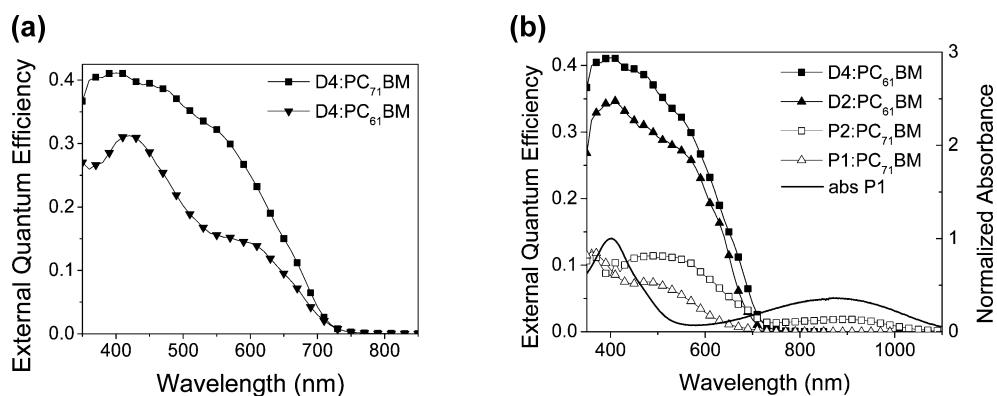


Figure 6. EQE characteristics of **D4** blended with PC_{61}BM or PC_{71}BM (1:3 ratio) (a), **D2**, **D4**, **P1**, and **P2** blended with PC_{71}BM (1:3 ratio) shown in comparison to the absorption spectrum of **P1** (b).

maxima of our reference all-thiophene dendrimer, **42T**, in apolar toluene and polar *o*-dichlorobenzene (ODCB) were found to be similar at 580 and 589 nm, respectively, demonstrating the minor effect of solvent polarity on the excited state. For dendrimers **D1** and **D3**, this however was not the case. **D1** in toluene displayed a maximum at 631 nm, whereas the same dendrimer in ODCB showed an emission maximum at 675 nm. It can therefore be concluded that this excited state displays charge-transfer character. Furthermore, we found a partial quenching of the fluorescence of **D1** in ODCB. On the other hand, for **D3**, we observe an emission maximum of the CT band in toluene at 662 nm, whereas the fluorescence is completely quenched in ODCB. From the fluorescence experiments, we can conclude that the band at low energies show a strong charge-transfer character, most probably between the dendrimer arms (3T moieties in **D1** and 5T

moieties in **D3**) and the pyrazinoquinoxaline core. It is likely that such a situation is not ideal for efficient electron transfer from the dendrimer core to a fullerene acceptor molecule in a solar cell device. This will be discussed further in another section.

Cyclic voltammetry (CV) was used to investigate the electrochemical properties of the dendrimers¹⁶ and polymers (see Figure S1). For example, the HOMO and LUMO energy levels of **P1** were calculated to be -5.3 and -4.0 eV, respectively, from the onset of the first oxidation and reduction wave. The energy levels of the TMS-protected DOTs, **D1** and **D3**, are represented in Figure 4. Because of the limited solubility of the deprotected dendrimers, **D2** and **D4**, CV could not be performed. We have previously shown that the HOMO/LUMO energy levels are not significantly altered upon removal of trimethylsilyl groups, and it is therefore expected that levels

Table 1. PV Device Results for the Pyrazinoquinoxaline Dendrimers and Polymers for Devices Made with PC₆₁BM

	D:A ratio	solvent	EQE	J_{SC} (mA/cm ²)	V_{OC} (V)	FF	PCE (%)
D1:PC ₆₁ BM	1:3	CB ^a	0.22	2.7	0.97	0.32	0.8
D2:PC ₆₁ BM	1:3	TCE ^b	0.26	2.7	0.84	0.30	0.7
D3:PC ₆₁ BM ¹⁶	1:3	CB	0.28	3.3	1.00	0.38	1.3
D4:PC ₆₁ BM	1:3	TCE	0.31	3.5	0.85	0.30	0.9
42T:PC ₆₁ BM ¹¹	1:3	CB	0.45	3.9	0.98	0.43	1.7

^aCB = chlorobenzene. ^bTCE = tetrachloroethane.

Table 2. PV Device Results for the Pyrazinoquinoxaline Dendrimers and Polymers for Devices Made with PC₇₁BM

	D:A ratio	solvent	EQE	J_{SC} (mA/cm ²)	V_{OC} (V)	FF	PCE (%)
D1:PC ₇₁ BM	1:3	CB ^a	0.34	4.8	0.91	0.33	1.4
D2:PC ₇₁ BM	1:3	TCE ^b	0.35	4.6	0.73	0.32	1.1
D3:PC ₇₁ BM	1:3	CB	0.35	4.9	0.98	0.35	1.7
D4:PC ₇₁ BM	1:3	TCE	0.41	5.6	0.87	0.32	1.6
P1:PC ₇₁ BM	1:4	CB	0.12	0.8	0.73	0.38	0.2
P2:PC ₇₁ BM	1:3	CB	0.10	2.2	0.54	0.63	0.8

^aCB = chlorobenzene. ^bTCE = tetrachloroethane.

for **D2** and **D4** are similar to those of **D1** and **D3**.¹⁰ Upon increasing generation size, it can be seen that the LUMO energy level is somewhat stabilized (−3.8 vs −3.9 eV) and that the HOMO energy level is to a larger extent destabilized (−5.7 vs −5.4 eV). **P1** displayed the lowest LUMO energy level (−4.0 eV) due to the electron-withdrawing strength of the trifluoromethyl groups relative to the weakly electron-donating ethylhexyl chains located at the 2-, 3-, 7-, and 8-positions of the pyrazinoquinoxaline moiety in **P2** (−3.8 eV). The electrochemical experiments further confirmed that the polymers have a smaller band gap than the dendrimers, supporting the results of the absorption experiments, which is also attributed to the different connectivities of the pyrazinoquinoxaline units to the thiophene moieties.

The dendrimers and polymers were tested in solution-processed bulk heterojunction solar cells with the following device structure: ITO|PEDOT:PSS|donor:PCBM|LiF|Al. The J – V and spectral response data are plotted in Figures 5 and 6, respectively, and summarized in Tables 1 and 2.

The TMS-containing dendrimers **D1** and **D3** displayed good solubility in common organic solvents such as CHCl₃, THF, and CB, whereas their TMS-free analogues **D2** and **D4** had very low solubility in these solvents. It was found that reasonable films for solar cells could only be made from hot solutions, in this case, when spin-coated from TCE at 80 °C. The first-generation TMS-protected dendrimers, **D1**, when blended with PC₆₁BM, displayed a short-circuit current density (J_{SC}) of 2.7 mA/cm², an open-circuit voltage (V_{OC}) of 0.97 V, and a fill factor (FF) of 0.32, leading to an overall power conversion efficiency of 0.8%. Devices based on **D2**:PC₆₁BM blends showed a J_{SC} of 2.7 mA/cm², which is similar to dendrimer **D1**, while the V_{OC} reduced to 0.84 V; the fill factor also reduced slightly to 0.30, and the overall PCE was found to be 0.7%. The second-generation TMS-protected dendrimer, **D3**, displayed a J_{SC} of 3.3 mA/cm², a V_{OC} of 1.00 V, and a fill factor of 0.38, resulting in a PCE of 1.3% when blended with PC₆₁BM. In comparison, the deprotected **D4** showed a small increase in J_{SC} to 3.5 mA/cm², a reduced V_{OC} (0.85 V), and a reduced fill factor (0.30), resulting in a PCE of 0.9%. Unlike the previously reported all-thiophene dendrimers, there is not a significant increase in the PCE of the devices after the removal of the trimethylsilyl groups. This is attributed to the reduced solubility

of the dendrimers after deprotection, which leads to poor film formation even when spin-coated from high temperatures. Although the replacement of the central bithiophene core with the pyrazinoquinoxaline unit resulted in a red-shift in the absorption profile,¹¹ which one would expect to result in increased charge generation in the solar cell and therefore an overall increase in PCE, this was not the case. The PV characteristics of the analogous all-thiophene dendrimer (**42T**)¹¹ were included in Table 1 for comparison with the **40T**-pyrazinoquinoxaline containing dendrimer (**D4**). Their differences in solar cell performance can be in part explained by the restricted rotational freedom of the planar pyrazinoquinoxaline core in comparison to the more flexible bithiophene core present in the **42T** dendrimer, which strongly influences the solubility of the molecules. On the other hand, fluorescence experiments (shown in Figure 3) indicated that the CT state localizes charge in the core of the dendrimers in polar media, which may also limit electron transfer to the fullerene acceptor. Furthermore, in the J – V curves of blends of the donor–acceptor dendrimers with PC₆₁BM one can see that the V_{OC} and fill factor are reduced upon deprotection (see Figure 5 and Table 1). **D4** displays a slightly higher short-circuit current density than **D3** (3.5 vs 3.3 mA/cm²). This is also reflected in the spectral response plot shown in Figure S2. In general, it can be seen that PV performance of the dendrimers blended with PC₆₁BM and PC₇₁BM display the same trends (see Tables 1 and 2). The main difference being that the magnitude of the current produced by the photovoltaic device is increased in the latter case due to absorption of PC₇₁BM in the visible region of the solar spectrum.²⁶

The two pyrazinoquinoxaline-based polymers were also tested in photovoltaic devices with the same structure as those for the dendrimers: ITO|PEDOT:PSS|donor:PCBM|LiF|Al. In the case of **P1**, the LUMO energy level was estimated to be equal to the LUMO of PC₆₁BM (−4.0 eV), as shown in Figure 4. Thus, for the polymer-based devices, we used PC₇₁BM as the electron acceptor due to its slightly lower LUMO energy level of (−4.1 eV).²⁵ For **P1**, the energy difference between the LUMOs of the donor and acceptor was calculated to be 0.1 eV, which turned out to be insufficient for efficient electron transfer from the polymer to the PC₇₁BM. This is clearly shown in Figure 6, where the plot of the spectral

response is compared with the absorption profile of **P1**. Since no current is generated where the polymer absorbs light (600–1100 nm), it has been concluded that electron transfer from **P1** to PC₇₁BM does not take place. The small amount of current that is generated in the photovoltaic cell is due to absorption by the acceptor, PC₇₁BM. The polymer plays a role in hole transport but not in charge generation, leading to an inefficient solar cell with PCE of 0.2% (Table 2).

Upon exchanging the electron-withdrawing CF₃ group by the weakly electron-donating 2-ethylhexyl side chains, the LUMO energy level of **P2** (−3.8 eV) increased relative to **P1** (−4.0 eV). This increase results in an energy difference of 0.3 eV between the LUMO of **P2** and the LUMO of PC₇₁BM, which should be sufficient for electron transfer from **P2** to the PC₇₁BM acceptor in the solar cell.^{27,28} **P2** displayed a *J*_{SC} of 2.2 mA/cm², a *V*_{OC} of 0.54 V, and a fill factor of 0.63, resulting in a PCE of 0.8% when blended with PC₇₁BM. Despite the high fill factor, the PCE was found to be limited by a low short-circuit current density. Figure 6 shows that **P2** does give a photoresponse up to the optical band gap at about 1.2 eV; however, attempts to further improve the *J*_{SC} by changing the processing conditions such as the solvent have been so far unsuccessful.

CONCLUSIONS

We report on the synthesis of pyrazinoquinoxaline-based dendrimers and polymers as well as we compare their optical, electrochemical, and photovoltaic properties. The different connectivities of the pyrazinoquinoxaline units to the thiophene moieties in the dendrimers (2,3,7,8-positions) and polymers (5,10-positions) led to a change in optical and electrochemical properties of these materials. This was apparent in the UV–vis absorption, i.e., the large difference in band gaps (1.7 eV for **D4** vs 1.2 eV for **P2**). Within the dendrimer series, we observe that the PV performance unexpectedly decreases upon removal of the solubilizing TMS groups. This finding was attributed to the poor film forming ability of **D2** and **D4** as well as to the electron-deficient core which can localize the charge transfer state in the center of the dendrimers. PCEs decreased from 1.7 to 1.6% for **D3** and **D4** blends with PC₇₁BM, respectively. Replacement of electron-withdrawing CF₃ groups on the pyrazinoquinoxaline moiety (**P1**) with weakly donating ethylhexyl chains (**P2**) raised the LUMO energy level from −4.0 to −3.8 eV. This allowed for electron transfer from **P2** to the PC₇₁BM acceptor in solar cell devices; however, the PCE of **P2**-based photovoltaic devices remained modest at 0.8%.

EXPERIMENTAL SECTION

Materials and Measurements. NMR spectra were recorded on a Bruker AMX 500 (¹H NMR: 500 MHz; ¹³C NMR 125 MHz) or a Bruker Avance 400 (¹H NMR: 400 MHz; ¹³C NMR 100 MHz), usually at 298 K, unless otherwise mentioned. Chemical shift values (δ) are given in ppm and were calibrated on residual nondeuterated solvent peaks (CDCl₃: ¹H NMR: 7.26 ppm, ¹³C NMR: 77.0 ppm; C₂D₂Cl₄: ¹H NMR: 6.00 ppm, ¹³C NMR: 74.0 ppm; CD₂Cl₂: ¹H NMR: 5.32 ppm, ¹³C NMR: 53.5 ppm; THF-*d*₆: ¹H NMR: 3.58 ppm, ¹³C NMR: 67.7 ppm) as internal standard. EI and CI mass spectroscopy were performed on a Finnigan MAT SSO-7000 or a Varian Saturn 2000 GCMS. MALDI-TOF spectra were recorded on a Bruker Daltonics Reflex III using dithranol or DCTB (*trans*-2-[3-(4-*tert*-butylphenyl)-2-methyl-2-propenylidene]malononitrile) as matrices. UV–vis absorption spectroscopy was carried out on a PerkinElmer Lambda 19 using Merck Uvasol grade solvents. The corrected fluorescence spectra were recorded on a PerkinElmer LS 55

fluorescence spectrometer of solutions with an optical density with less than 0.1. Cyclic voltammetry experiments were performed with a computer-controlled EG&G PAR 273 potentiostat and a three-electrode single-compartment cell with a platinum working electrode, a platinum wire counter electrode, and an Ag/AgCl reference electrode. All potentials were internally referenced to the ferrocene/ferrocenyl couple (−5.1 eV). Elemental analyses were performed on an Elementar Vario EL. Plastic sheets precoated with silica gel, Merck Si60 F254, were used for thin layer chromatography. Glass columns packed with Merck Silica 60, mesh 0.063–0.2 μ m, were used for column chromatography. Size-exclusion chromatography was performed on a glass column packed with biorad beads SX-1 swollen in dichloromethane. Dichloromethane was used as the eluent. Molecular weight determinations were performed using gel permeation chromatography (HPLC pump from Dionex) calibrated against polystyrene standards. Polymers were eluted with THF using a flow rate of 1 mL/min and monitored with a UV–vis detector (Waters 486 at 254 nm). Solvents were purchased at ProLabo and distilled prior to use. Commercially available 2,2'-thenyl **1** (Alfa Aesar, 98%) and 1,2,4,5-tetraaminobenzene tetrahydrochloride (Aldrich, techn.) were used. Dendrimers **D1** and **D3** were prepared as described in the literature.¹⁶

Device Fabrication. Photovoltaic devices were made by spin-coating PEDOT:PSS (Clevios P, VP Al4083) onto precleaned, patterned indium tin oxide (ITO) substrates (14 Ω /square) (Naranjo Substrates). The photoactive layer (ca. 80 nm) was deposited by spin-coating from a mixed solution of dendrimers **D1–D4** or **P1–P2** with PC₆₁BM or PC₇₁BM (1:3 ratio w/w, β = 25 mg/mL in chlorobenzene or β = 15 mg/mL in 1,1,2,2-tetrachloroethane (TCE)). The active layers spin-coated from TCE were done from hot solutions at 80 °C and substrates heated to 100 °C. PC₆₁BM and PC₇₁BM were purchased from Solenne BV, Netherlands, 99% pure. The counter electrode of LiF (1 nm) and aluminum (100 nm) was deposited by vacuum evaporation at 3 \times 10^{−7} mbar. The active areas of the cells were 0.09 or 0.16 cm². *J–V* characteristics were measured under ~100 mW/cm² white light from a tungsten–halogen lamp filtered by a Schott GG385 UV filter and a Hoya LB120 daylight filter, using a Keithley 2400 source meter. Short circuit currents under AM1.5G conditions were obtained from the spectral response and convolution with the solar spectrum.²⁹ Spectral response was measured under operation conditions using bias light from a 532 nm solid state laser (Edmund Optics). Monochromatic light from a 50 W tungsten halogen lamp (Philips focusline) in combination with monochromator (Oriel, Cornerstone 130) was modulated with a mechanical chopper. The response was recorded as the voltage over a 50 Ω resistance, using a lock-in amplifier (Stanford Research Systems SR830). A calibrated Si cell was used as reference. The device was kept behind a quartz window in a nitrogen-filled container.

Synthesis of Dendrimers and Polymers. 2,3,7,8-Tetrakis((5'-(thien-2-yl)-2,2':4',2''-terthien-5-yl))-pyrazino[2,3-*g*]quinoxaline (**D2**). 2,3,7,8-Tetrakis((5'-(5-trimethylsilylthien-2-yl)-5''-trimethylsilyl-2,2':4',2''-terthien-5-yl))-pyrazino[2,3-*g*]quinoxaline (**D1**) (72 mg, 0.035 mmol) was dissolved in tetrachloroethane (10 mL), to which 20 mL of acetic acid was added. The reaction mixture was heated to 130 °C for 4 days. Then the mixture was poured into water and extracted with TCE. The organic layer was washed with water three times, followed by washing with Na₂CO₃ solution and finally saturated NaCl solution. The organic layer was dried over sodium sulfate. Because of low solubility of the product, the filtrand was subjected to Soxhlet extraction with TCE for 24 h, after which the solvent reduced in volume. The obtained solid was washed with pentane (3 \times 10 mL) and methanol (3 \times 10 mL) and dried under vacuum to give 50 mg (95%) of **D2** as a black solid. ¹H NMR (C₂D₂Cl₄, 500 MHz 100 °C): δ (ppm) 8.78 (s, 2H, PQ-H), 7.56 (d, *J*₁ = 1.18 Hz, 4H), 7.45 (s, 4H), 7.39–7.36 (dd, *J*₁ = 1.17 Hz, *J*₂ = 3.60 Hz, 8H), 7.27 (d, *J*₁ = 1.18 Hz, 4H), 7.23 (d, 4H), 7.19 (d, 4H), 7.10–7.07 (m, 8H). MS (MALDI-TOF, dithranol): *m/z* = 1494.0 [M⁺].

2,3,7,8-Tetrakis-[5'-(thien-2-yl)-2,2':4',2''-terthien-5-yl])-5'''-(thien-2-yl)-2,2':4',2''-S''':2''':4''':2''''-quinquethien-5-yl]pyrazino[2,3-*g*]quinoxaline (**D4**). 2,3,7,8-Tetrakis-[5'-(5'-(5-trimethylsilylthien-2-yl)-

5''-trimethylsilyl-2,2':4',2''-terthien-5-yl)-5'''-(5-trimethylsilylthien-2-yl)-5''''-(trimethylsilyl)-2,2':4',2''':5'',2''':4''',2''''-quinquethien-5-yl]-pyrazino[2,3-g]quinoxaline (**D3**) (80 mg, 0.017 mmol) was dissolved in tetrachloroethane (10 mL, to which 20 mL of acetic acid was added). The reaction mixture was heated to 130 °C for 3 days. Then the mixture was poured into water and extracted with TCE. The organic layer was washed with water three times, followed by washing with Na₂CO₃ solution and finally saturated NaCl solution. The organic layer was dried over sodium sulfate. Because of low solubility of the product, the filtrand was subjected to Soxhlet extraction with TCE for 24 h, after which the solvent reduced in volume. The obtained solid was washed with pentane (3 × 10 mL) and methanol (3 × 10 mL) and dried under vacuum to give 57 mg (95%) of **D4** as a black solid. ¹H NMR (C₂D₂Cl₄, 500 MHz 100 °C): δ (ppm) 8.78 (s, 2H, PQ-H), 7.58 (d, J₁ = 1.18 Hz, 4H), 7.47 (s, 4H), 7.36–7.31 (m, 16H), 7.29 (s, 4H), 7.27 (s, 4H), 7.22–7.18 (m, 28H), 7.13 (d, 8H), 7.06–7.03 (m, 16H). MS (MALDI-TOF, DCTB): *m/z* = 3462.0 [M⁺].

4,4'-Bis(trifluoromethyl)benzyl (**1**). To a solution of 4-bromobenzotrifluoride (3 g, 13.3 mmol) in 12.5 mL of dry THF was added 5.08 mL of *n*-BuLi (2.5 M in hexanes, 12.7 mmol) using a syringe at –78 °C. After stirring at –78 °C for 1 h, the mixture was transferred to a suspension of 1,4-dimethylpiperazine-2,3-dione (0.86 g, 6.06 mmol) in 12.5 mL of dry THF dropwise via a cannula under argon at –78 °C. The reaction mixture was allowed to gradually come to room temperature. After 3 days, the reaction was hydrolyzed with 100 mL of 10% HCl and extracted with CH₂Cl₂. The organic layer was dried over sodium sulfate and reduced in volume. The product was purified by column chromatography (silica gel, petroleum ether:CH₂Cl₂ 5:1 v/v) to give a yellow solid (1.65 g, 79%). ¹H NMR (CDCl₃, 400 MHz): δ (ppm) 3.53 (s, 4H), 3.03 (s, 6H).

2,3,7,8-Tetra(4'-trifluoromethylphenyl)pyrazino[2,3-g]quinoxaline (**2**). **1** (0.5 g, 1.44 mmol) and 1,2,4,5-benzenetetraamine tetrahydrochloride (0.205 g, 0.72 mmol) were dissolved in 20 mL of degassed *n*-butanol. The reaction mixture was heated to 120 °C for 16 h. After cooling to room temperature, the mixture was poured into 100 mL of water and extracted with CH₂Cl₂. The organic layer was washed with water (2×), Na₂CO₃ solution (1×), and NaCl solution (1×) and finally dried over sodium sulfate. The solvent was removed and purification was done using column chromatography (silica gel, petroleum ether:CH₂Cl₂ 1:1) to yield an orange solid (0.46 g, 85%). ¹H NMR (CDCl₃, 400 MHz): δ (ppm) 9.09 (s, 2H), 7.75 (d, 8H), 7.71 (d, 8H).

5,10-Dibromo-2,3,7,8-tetra(4'-trifluoromethylphenyl)pyrazino[2,3-g]quinoxaline (**3**). Pyrazinoquinoxaline **2** (154 mg, 0.2 mmol) was combined with NaHCO₃ (68 mg, 0.81 mmol) in 5 mL of CHCl₃. The solution was cooled to 0 °C, and Br₂ (130 mg, 0.81 mmol) was added. The reaction flask was sealed and heated to 80 °C for 4 h. After cooling, the reaction mixture was put directly on a silica gel column (petroleum ether:EA 1:0.05). The product was further purified by recrystallization from a mixture of THF/pentane to obtain fluffy orange crystals (173 mg, 95%). ¹H NMR (CDCl₃, 400 MHz): δ (ppm) 7.90 (d, 8H), 7.74 (d, 8H). ¹³C NMR (THF-*d*₈, 100 MHz): δ (ppm) 155.07, 142.56, 139.71, 132.03, 126.35, 126.31, 123.88. MS (MALDI-TOF, dithranol): *m/z* = 838.3 [M⁺–Br], 915.2 [M⁺].

5,10-Dithienyl-2,3,7,8-tetra(4'-trifluoromethylphenyl)pyrazino[2,3-g]quinoxaline (**4**). **3** (0.6 g, 0.65 mmol) was combined with 2-tributylstannylthiophene in 20 mL of dry DMF. The reaction mixture was degassed, followed by addition of Pd(PPh₃)₂Cl₂ (23 mg, 0.033 mmol). The reaction was heated to 70 °C and allowed to react 24 h. Upon cooling the mixture was poured into water and extracted with CH₂Cl₂. The organic phase was washed with water (2×), Na₂CO₃ solution (1×), and NaCl solution (1×) and finally dried over sodium sulfate. The solvent was reduced in volume, and product was precipitated in methanol to yield a blue solid (0.52 g, 86%). ¹H NMR (CDCl₃, 400 MHz): δ (ppm) 8.37 (d, 2H), 7.91 (d, 8H), 7.80 (d, 2H), 7.71 (d, 8H), 7.40 (dd, 2H). ¹³C NMR (THF-*d*₈, 125 MHz): δ (ppm) 152.51, 143.23, 137.87, 135.80, 135.13, 132.16, 131.71, 130.48, 127.18, 126.46, 124.37. MS (MALDI-TOF, DCTB): *m/z* = 922.2 [M⁺].

5,10-(Bis(5-bromothiien-2-yl)-2,3,7,8-tetra(4-trifluoromethylphenyl)pyrazino[2,3-g]quinoxaline (**5**). **4** (0.265 g, 0.29 mmol) was dissolved in 10 mL of THF, to which *N*-bromosuccinimide (0.112 g, 0.63 mmol) was added. The reaction was stirred at room temperature for 24 h, after which it was precipitated in methanol, collected using a centrifuge, and dried under vacuum to yield a green solid (0.265 g, 85%). ¹H NMR (THF-*d*₈, 400 MHz): δ (ppm) 8.49 (d, 2H), 7.98 (d, 8H), 7.83 (d, 8H), 7.35 (d, 2H). ¹³C NMR (THF-*d*₈, 100 MHz): δ (ppm) 153.07, 144.92, 137.63, 137.13, 136.77, 132.29, 130.74, 129.15, 126.60, 124.12, 120.30. MS (MALDI-TOF, DCTB): *m/z* = 1080.1 [M⁺].

Polymer (**P1**). 2,5''-Distannyl-3,4,3'',4''-tetrabutylterthiophene (111 mg, 0.138 mmol) was added to a dry 25 mL two-necked flask, which was evacuated and purged with argon (2×) before addition of **5** (150 mg, 0.138 mmol). A mixture of toluene and DMF (4:1, 10 mL) was added to the flask followed by further degassing using argon. After 10 min, Pd(PPh₃)₄ (7 mg, 0.007 mmol) was added to the reaction mixture followed by further degassing for another 15 min. The reaction was heated to 120 °C and allowed to react for 24 h. Upon cooling the crude product was precipitated in methanol and underwent successive Soxhlet extraction in methanol, acetone, hexane, and THF. The THF fraction was then reprecipitated in methanol and dried under vacuum to yield **P1** (97 mg) in 48% yield. ¹H NMR (THF-*d*₈, 400 MHz): δ (ppm) 8.75 (broad, 2H), 8.07 (broad, 8H), 7.84 (broad, 8H), 7.50 (broad, 2H), 7.28 (broad, 2H), 2.92 (broad, 8H), 1.56–1.29 (m, 16H), 0.89 (m, 6H). *M_n* = 6300 g/mol, *M_w* = 8900 g/mol, and PDI = 1.4.

1-Bromo-4-(2'-ethylhexyl)benzene (**6**). To a suspension of Mg (0.936 g, 0.038 mol) in dry diethyl ether (5 mL), 1-bromo-2-ethylhexane (7.5 g, 0.039 mol) dissolved in 30 mL of dry diethyl ether was added dropwise at 50 °C. The reaction was allowed to react for 12 h and was then transferred to a dropping funnel attached to a three-necked flask containing ZnBr₂ (8.74 g, 0.039 mol) in 20 mL of dry THF. The reaction mixture was cooled to 0 °C, and the Grignard reagent was added dropwise. Instantaneously, a white precipitate was formed, and an additional 25 mL of dry diethyl ether was added so the slurry could be stirred. 1-Bromo-4-iodobenzene (10.98 g, 0.039 mol) was dissolved in 60 mL of dry diethyl ether and added dropwise to the reaction mixture via the dropping funnel. Pd(dppf)Cl₂ (420 mg, 0.51 mmol) then added to the mixture, followed by heating to 55 °C for 16 h, at which point the remainder of the catalyst was added (210 mg, 0.26 mmol) and the reaction was allowed to proceed at 55 °C for 24 h. Upon cooling to room temperature, 20 mL of HCl (1 M) was added to the reaction mixture. More diethyl ether was added, and the organic phase was washed with water (3×) and NaCl solution (1×) and finally dried over sodium sulfate. The solvent was reduced in volume, and crude product was purified using multiple sublimations (12 mbar, 60 °C), isolating a white solid which was identified as the 1-bromo-4-iodobenzene starting material. The remaining liquid was purified using column chromatography (silica gel, petroleum ether) to yield a colorless liquid (3.7 g, 36%). ¹H NMR (CDCl₃, 400 MHz): δ (ppm) 7.37 (d, 2H), 7.02 (d, 2H), 2.49 (d, 2H), 1.54 (broad, 1H), 1.26 (m, 8H), 0.86 (m, 6H). ¹³C NMR (CDCl₃, 100 MHz): δ (ppm) 140.81, 131.08, 130.91, 119.19, 40.99, 39.46, 32.19, 28.77, 26.28, 22.99, 14.12, 10.73. GC-MS: *m/z* 268 [M]⁺.

1,2-Bis(4-(2'-ethylhexyl)phenyl)-1,2-ethanedione (**7**). 1-Bromo-4-(2'-ethylhexyl)benzene (**6**) (3.5 g, 13 mmol) was added to a two-necked flask. After the addition of THF (12.5 mL), *n*-butyllithium (4.96 mL, 2.5 M, 12.4 mmol) was added dropwise at –78 °C. To a suspension of piperazine in 12.5 mL of dry THF, the lithiated reactant was added dropwise with a canule over several minutes at –78 °C. The reaction mixture was then slowly allowed to come to room temperature. The next day, 100 mL of HCl (10% v/v) was added to the reaction mixture, and the product was extracted with CH₂Cl₂. The organic phase was washed with water (2×) and NaCl solution (1×) and finally dried over sodium sulfate. The solvent was reduced in volume to yield an orange liquid, which was further purified using column chromatography (silica gel, petroleum ether:CH₂Cl₂, 2:1). The product was collected as a yellow oil (2.15 g, 84%). ¹H NMR (CDCl₃, 400 MHz): δ (ppm) 7.88 (d, 4H), 7.29 (d, 4H), 2.60 (d,

4H), 1.61 (s, 2H), 1.27 (m, 16H), 0.87 (t, 12H). ^{13}C NMR (CDCl_3 , 100 MHz): δ (ppm) 194.53, 150.20, 130.76, 129.89, 129.78, 40.98, 40.42, 32.27, 28.75, 25.37, 22.96, 14.11, 10.70. MS (CI): $m/z = 934.0$ [M]. Elemental analysis calcd for $\text{C}_{30}\text{H}_{42}\text{O}_2$: C: 82.90%, H: 9.74%. Found: C: 82.76%, H: 9.59%.

2,3,7,8-Tetra(4'-ethyl-2''-hexylphenyl)pyrazino[2,3-g]quinoxaline (8). 7 (0.250 g, 0.57 mmol) and 1,2,4,5-benzenetetraamine tetrahydrochloride (82 mg, 0.29 mmol) were dissolved in 20 mL of degassed acetic acid. The reaction mixture was heated to 125 °C for 24 h. After cooling to room temperature, the mixture was poured into 100 mL of water and extracted with diethyl ether. The organic layer was washed with water (2X), Na_2CO_3 solution (1X), and NaCl solution (1X) and finally dried over sodium sulfate. The solvent was removed, and purification was done using column chromatography (silica gel, petroleum ether: CH_2Cl_2 , 1:0 \rightarrow 1:1) to yield a yellow solid (0.40 g, 74%). ^1H NMR ($\text{THF}-d_8$, 400 MHz): δ (ppm) 8.86 (s, 2H), 7.60 (d, 8H), 7.21 (d, 8H), 2.63 (d, 8H), 1.67 (m, 4H), 1.36 (m, 32H), 0.95 (t, 24H). ^{13}C NMR (CDCl_3 , 100 MHz): δ (ppm) 155.36, 143.48, 140.31, 136.15, 129.72, 129.08, 128.40, 41.09, 39.99, 32.30, 28.84, 25.46, 23.03, 14.16, 10.84. MS (MALDI-TOF, dithranol): $m/z = 936.0$ [M $^+$]. Elemental analysis calcd. for $\text{C}_{66}\text{H}_{86}\text{N}_4$: C: 84.74%, H: 9.27%, N: 5.99%. Found: C: 84.83%, H: 9.38%, N: 5.71%.

5,10-Dibromo-2,3,7,8-tetra(4'-ethyl-2''-hexylphenyl)pyrazino[2,3-g]quinoxaline (9). Pyrazinoquinoxaline 8 (250 mg, 0.27 mmol) was combined with NaHCO_3 (45 mg, 0.53 mmol) in 5 mL of CHCl_3 . The solution was cooled to 0 °C, and Br_2 (85 mg, 0.53 mmol) was added. The reaction flask was sealed and heated to 80 °C for 24 h. After cooling, an additional 1 equiv of Br_2 (42 mg) and NaHCO_3 (23 mg) was added to the reaction flask and allowed to further react at 50 °C for 6 h. The reaction mixture was put directly on a silica gel column (petroleum ether: CH_2Cl_2 , 10:3). The product was further purified by recrystallization from a mixture of methanol/dichloromethane to obtain fluffy yellow crystals (132 mg, 45%). ^1H NMR (CDCl_3 , 400 MHz): δ (ppm) 7.69 (d, 8H), 7.21 (d, 8H), 2.61 (d, 8H), 1.65 (m, 4H), 1.33 (m, 32H), 0.92 (t, 24H). ^{13}C NMR (CDCl_3 , 100 MHz): δ (ppm) 156.21, 145.10, 139.56, 137.12, 131.39, 130.06, 125.07, 42.39, 41.08, 33.60, 30.06, 28.69, 24.24, 14.82, 11.48. (MALDI-TOF, dithranol): $m/z = 1013$ [M $^+$ -Br], 1094 [M $^+$]. Elemental analysis calcd. for $\text{C}_{66}\text{H}_{84}\text{Br}_2\text{N}_4$: C: 72.51%, H: 7.74%, N: 5.12%. Found: C: 72.32%, H: 7.66%, N: 5.03%.

Polymer P2. 2,5''-Distannylbithiophene (18 mg, 0.036 mmol) was added to a dry 25 mL two-necked flask, which was evacuated and purged with argon (2X) before addition of 9 (40 mg, 0.036 mmol). Toluene (2.5 mL) was added to the flask followed by further degassing using argon. After 10 min, $\text{Pd}_2(\text{dba})_3$ (1.7 mg, 0.002 mmol) and $\text{P}(o\text{-tolyl})_3$ (3.4 mg, 0.011) were added to the reaction mixture followed by further degassing for another 15 min. The reaction was heated to 100 °C and allowed to react for 60 h. Upon cooling the crude product was precipitated in methanol and underwent successive Soxhlet extraction in methanol, acetone, hexane, and THF. The THF fraction was then reprecipitated in methanol and dried under vacuum to yield P1 (39 mg) in 95% yield. ^1H NMR ($\text{THF}-d_8$, 400 MHz): δ (ppm) 8.81 (broad s, 2H), 7.86 (broad s, 8H), 7.66 (broad s, 2H), 7.22 (broad s, 8H), 2.58 (broad s, 8H), 1.63 (broad s, 4H), 1.28 (broad s, 32H), 0.85 (broad s, 24H). $M_n = 53\,000$ g/mol, $M_w = 113\,000$ g/mol, and PDI = 2.1.

■ ASSOCIATED CONTENT

● Supporting Information

Figures S1 and S2. This material is available free of charge via the Internet at <http://pubs.acs.org>.

■ AUTHOR INFORMATION

Corresponding Author

*E-mail gisela.schulz@uni-ulm.de (G.L.S.), peter.baeuerle@uni-ulm.de (P.B.); Fax (+49) 731-502-2840.

Present Address

[§]Chang-Qi Ma: Printable Electronic Research Center, Suzhou Institute of Nano-Tech and Nano-Bionics, Chinese Academy of Sciences, 398 Ruoshui Road SEID SIP, Suzhou 215123, P. R. China.

Notes

The authors declare no competing financial interest.

■ ACKNOWLEDGMENTS

We thank the Dutch Polymer Institute (program no. 661) for financial support as well as Mike Wendel (University of Ulm) for performing the polymer molecular weight determinations.

■ REFERENCES

- (1) Spanggaard, H.; Krebs, F. C. *Sol. Energy Mater. Sol. Cells* **2004**, *83*, 125–146.
- (2) Gunes, S.; Neugebauer, H.; Sariciftci, N. S. *Chem. Rev.* **2007**, *107*, 1324–1338.
- (3) Boudreault, P.-L.; Najari, A.; Leclerc, M. *Chem. Mater.* **2011**, *23*, 456–469.
- (4) Mishra, A.; Bäuerle, P. *Angew. Chem., Int. Ed.* **2012**, *51*, 2020–2067.
- (5) Cheng, Y.-J.; Yang, S.-H.; Hsu, C.-S. *Chem. Rev.* **2009**, *109*, 5868–5923.
- (6) Cravino, A.; Leriche, P.; Alévêque, O.; Roquet, S.; Roncali, J. *Adv. Mater.* **2006**, *18*, 3033–3037.
- (7) Zhang, J.; Deng, D.; He, C.; He, Y.; Zhang, M.; Zhang, Z.-G.; Zhang, Z.; Li, Y. *Chem. Mater.* **2010**, *23*, 817–822.
- (8) Rance, W. L.; Rupert, B. L.; Mitchell, W. J.; Köse, M. E.; Ginley, D. S.; Shaheen, S. E.; Rumbles, G.; Kopidakis, N. *J. Phys. Chem. C* **2010**, *114*, 22269–22276.
- (9) Sun, X. B.; Zhou, Y. H.; Wu, W. C.; Liu, Y. Q.; Tian, W. J.; Yu, G.; Qiu, W. F.; Chen, S. Y.; Zhu, D. B. *J. Phys. Chem. B* **2006**, *110*, 7702–7707.
- (10) Ma, C.-Q.; Mena-Osteritz, E.; Debaerdemaeker, T.; Wienk, M. M.; Janssen, R. A.; Bäuerle, P. *Angew. Chem., Int. Ed.* **2007**, *46*, 1679–1683.
- (11) Ma, C.-Q.; Fonrodona, M.; Schikora, M. C.; Wienk, M. M.; Janssen, R. A. J.; Bäuerle, P. *Adv. Funct. Mater.* **2008**, *18*, 3323–3331.
- (12) Fischer, M. K. R.; López-Duarte, I.; Wienk, M. M.; Martínez-Díaz, M. V.; Janssen, R. A. J.; Bäuerle, P.; Torres, T. s. *J. Am. Chem. Soc.* **2009**, *131*, 8669–8676.
- (13) Mishra, A.; Ma, C. Q.; Janssen, R. A. J.; Bäuerle, P. *Chem.—Eur. J.* **2009**, *15*, 13521–13534.
- (14) Fischer, M. K. R.; Kaiser, T. E.; Wurthner, F.; Bäuerle, P. *J. Mater. Chem.* **2009**, *19*, 1129–1141.
- (15) Tam, T. L.; Zhou, F.; Li, H.; Yu Pang, J. C.; Lam, Y. M.; Mhaisalkar, S. G.; Su, H.; Grimsdale, A. C. *J. Mater. Chem.* **2011**, *21*, 17798–17804.
- (16) Mastalerz, M.; Fischer, V.; Ma, C. Q.; Janssen, R. A. J.; Bäuerle, P. *Org. Lett.* **2009**, *11*, 4500–4503.
- (17) Zhang, F.; Bijleveld, J.; Perzon, E.; Tvingstedt, K.; Barrau, S.; Inganäs, O.; Andersson, M. R. *J. Mater. Chem.* **2008**, *18*, 5468–5474.
- (18) Zoombelt, A. P.; Fonrodona, M.; Turbiez, M. G. R.; Wienk, M. M.; Janssen, R. A. J. *J. Mater. Chem.* **2009**, *19*, 5336–5342.
- (19) Wang, E. R.; Hou, L. T.; Wang, Z. Q.; Hellstrom, S.; Mammo, W.; Zhang, F. L.; Inganäs, O.; Andersson, M. R. *Org. Lett.* **2010**, *12*, 4470–4473.
- (20) Unver, E. K.; Tarkuc, S.; Baran, D.; Tanyeli, C.; Toppare, L. *Tetrahedron Lett.* **2011**, *52*, 2725–2729.
- (21) Peng, Q.; Liu, X. J.; Qin, Y. C.; Xu, J.; Li, M. J.; Dai, L. M. *J. Mater. Chem.* **2011**, *21*, 7714–7722.
- (22) Marder, S.; Cho, J.-Y.; Barlow, S.; Kippelen, B.; Domercq, B. WO 2005123754, 2005.
- (23) Lenes, M.; Wetzelaer, G.-J. A. H.; Kooistra, F. B.; Veenstra, S. C.; Hummelen, J. C.; Blom, P. W. M. *Adv. Mater.* **2008**, *20*, 2116–2119.

- (24) Hummelen, J. C.; Knight, B. W.; LePeq, F.; Wudl, F.; Yao, J.; Wilkins, C. L. *J. Org. Chem.* **1995**, *60*, 532–538.
- (25) Xie, Q. S.; Arias, F.; Echegoyen, L. *J. Am. Chem. Soc.* **1993**, *115*, 9818–9819.
- (26) Wienk, M. M.; Kroon, J. M.; Verhees, W. J. H.; Knol, J.; Hummelen, J. C.; van Hal, P. A.; Janssen, R. A. J. *Angew. Chem., Int. Ed.* **2003**, *42*, 3371–3375.
- (27) Koster, L. J. A.; Mihailetschi, V. D.; Blom, P. W. M. *Appl. Phys. Lett.* **2006**, *88*, 093511.
- (28) Scharber, M. C.; Muehlbacher, D.; Koppe, M.; Denk, P.; Waldauf, C.; Heeger, A. J.; Brabec, C. J. *Adv. Mater.* **2006**, *18*, 789–794.
- (29) Wienk, M. M.; Turbiez, M.; Gilot, J.; Janssen, R. A. J. *Adv. Mater.* **2008**, *20*, 2556–2560.